Available online at www.sciencedirect.com
ScienceDirect
Trans. Nonferrous Met. Soc. China 25(2015) 2856−2865
Transactions of Nonferrous Metals Society of China
www.tnmsc.cn

Effect of small tool pin profiles on microstructures and mechanical properties of 6061 aluminum alloy by friction stir welding

H. I. DAWOOD[1,2], Kahtan S. MOHAMMED[1], Azmi RAHMAT[1], M. B. UDAY[3]

1. School of Materials Engineering, Universiti Malaysia Perlis, Taman Muhibah-Jejawi-Arau, Perlis 02600, Malaysia;
2. Department of Chemical Engineering, College of Engineering, University of AL-Qadisiya, AL-Qadisiya, Iraq;
3. Centre for Low Carbon Transport in Cooperation with Imperial College London,
Institute for Vehicle System Engineering, Universiti Teknologi Malaysia, Skudai 81310, Malaysia

Received 20 October 2014; accepted 29 June 2015

Abstract: The effect of small tool pin profiles on the microstructures and mechanical properties of 6061 aluminum alloy joints using friction stir welding (FSW) technique was investigated. Three different tool pin profiles: threaded tapered cylindrical (T_1), triangular (T_2) and square (T_3) were used to produce the joints. The results indicate that the weld joints are notably affected by joining with different tool pin profiles. The triangular tool pin profile produces the best metallurgical and mechanical weld properties compared with other tool pin profiles. Besides, the lowest tensile strength and microhardness are obtained for the joint friction stir welded with square tool pin profile. It is observed that the smaller tool pin profile and shoulder diameter lead to narrow region of heat affected zone (HAZ) and a desired level of softening. The fracture surface examination shows that the joints are also affected when welding with different types of tool pin profiles. The fracture surface shows that the triangular specimen fails with a ductile fracture mode during the tensile test, while the brittle fracture modes are observed in the joints fabricated with other tool pin profiles (T_1 and T_3).
Key words: friction stir welding; small tool pin profile; mechanical properties; aluminum alloy; grain size

1 Introduction

Friction stir welding (FSW) is a solid state welding process in which the relative motion between the welding tool and the workpieces produces heat. This makes the material soft, and therefore it can be joined by plastic deformation diffusion. This method relies on the direct conversion of mechanical energy to thermal energy forming the weld joint without any external source of heat [1]. In the FSW process, a non-consumable rotating tool is forced down into the joint line under conditions where the frictional heating is sufficient to raise the temperature of the workpieces. It can plastically deform and locally plasticize. In the FSW technique, there is no liquid state of the material, and the weld takes place in the solid phase under the melting point of the material [2]. Thus, all the problems related to the solidification of a fused material are avoided.

Tool pin profile is a very important factor for producing sound and defect free welds. The optimization of FSW tool pin geometry plays an active role in increasing the quality of the weld [3]. During this process, the material undergoes an intense plastic deformation at elevated temperature, resulting in a significant grain refinement in the nugget zone (NZ). This phenomenon is known as dynamic recrystallization [4]. The tool geometry, in particular the pin profile, is a predominant factor in determining the weld geometry, localized heating, and stirring action. However, the behaviour of material flow is predominantly influenced by the tool pin profile, tool pin dimensions and FSW process parameters [5]. ELANGOVAN et al [6] studied the influences of tool pin profile and welding speed on the behaviour of material flow and the quality of the weld. They reported that the tool pin profile plays a major role in deciding the quality of the weld. However, very little attention has been paid to the effect of pin profile on the distribution of particles [7, 8].

The grain refinement by FSW in alloys has been reported by several researchers [9−15]. It has been demonstrated that the grain structures depend heavily on the processing conditions, including processing parameters, tool geometry and cooling rate. However, a

Corresponding author: H. I. DAWOOD; Tel: +60-17-4489057; Fax: +60-04-9798178; E-mail: hassanissa1972@gmail.com
DOI: 10.1016/S1003-6326(15)63911-5

recent research has also uncovered several complexities and special features of the material flow in FSW such as the lack of mixing the plasticized materials on atomic scale and the formation of certain interesting patterns which still require further work. Besides, no effort has been devoted to study the effects of small tool pin profiles on the NZ formation. Accordingly, the objective of this study is to investigate the effect of small tool pin profiles and small unchanged shoulder diameter on the microstructures and mechanical properties of 6061 aluminum alloy joints. Moreover, small pin dimensions are recommended to fabricate a weld joint which has a plate thickness of 4 mm or less, because the plate thicknesses more than 4 mm lead to break pins.

2 Experimental

6061 aluminum alloy was used with the chemical composition: 97.57% Al, 0.525% Si, 0.339% Fe, 1.062% Mg, 0.120% Cu and 0.080% Mn. The material was supplied by a local supplier (Heap Sing Huat Metal and Machinery Sdn Bhd). The aluminum plate with a thickness of 4 mm was sliced into the required sizes (210 mm × 100 mm) using a cutting band saw machine (UE−712A). Three pairs of aluminum alloy strip were coupled in a butt joint configuration paralleling to the rolling direction of the plates and clamped rigidly on the backing plate. Before the FSW process, the surfaces of plates were cleaned using acetone to remove the dirt and grease.

The FSW was carried out on a vertical milling machine, type KAMA (X6325; 3Hp; TRPER R8; 30 KN). The axial force was measured using a load cell and found approximately equal to 7.5 kN. The FSW tools were designed and manufactured from medium carbon steel and were heat-treated to about HRC 58. The chemical composition of the welding tool is shown in Table 1. Three FSW tools with different pin geometries denoted as T_1, T_2 and T_3 were employed, and the profiles are shown in Fig. 1. The T_1, T_2, and T_3 pin were inscribed in a circle with a diameter of 2 mm and each tool pin had a length of 3.7 mm. A tool shoulder had a diameter of 9 mm. The welding tool rotated in a clockwise direction at a constant rotational speed of 1750 r/min. The rotating tool traversed at a speed of 60 mm/min along the weld line perpendicular to the rolling direction. However, these values for traverse and rotation speeds were considered to be the best parameters obtained experimentally during the FSW process. The single pass welding procedure was followed to fabricate the joints. The FSW produced an asymmetric microstructure representing the advancing side (AS) and retreating side (RS). The AS is the side in which the velocity vector of rotational speed is in the same direction with the welding speed and the other side represents the RS.

Table 1 Chemical composition of welding tool (mass fraction, %)

C	Mn	P	Fe
0.44	0.79	0.012	Bal.

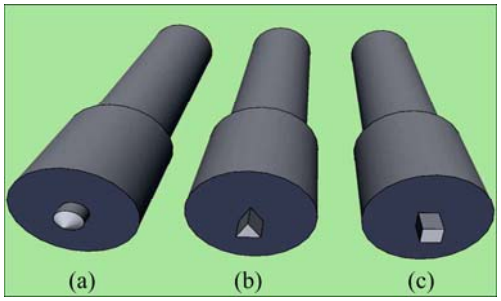

Fig. 1 Tool pin geometries: (a) Threaded tapered cylindrical pin T_1, (b) Triangular pin T_2; (c) Square pin T_3

Four welds were fabricated for each parameter test in order to ensure the accuracy and repeatability of results. The best possible welded sample was then selected from each parameter test-set based on the criteria of visual inspection to evaluate the welds. A continuous and visual defect free weld seam was required. Three specimens of each weld, from the beginning, middle, and end of the weld, were considered for each mechanical test.

A microstructural analysis was performed on the cross section perpendicular to the welding direction. The specimens for metallographic examination were sectioned to the required sizes and ground to a smooth surface using different abrasive papers (180−1500). The final polishing was performed using the diamond paste solution with the particle size of 0.5 μm. The microstructure of specimens was revealed through inundation etching in Keller's reagent (2 mL HF + 5 mL HNO_3 + 3 mL HCl + 190 mL H_2O). The microstructure of the specimens was examined by field emission scanning electron microscopy (FESEM) (ZEISS SUPRA 35VP). The welding samples of 6061 aluminum alloy were also analyzed using a D8 Advance X-ray diffractometer (Bruker Analytical X-ray Systems), using a copper target to identify the phases in the welded joints. For the tensile tests, the FSW plates were machined according to ASTM: E8/E8M−11 perpendicularly to the welding direction. The tensile testing was carried out on an INSTRON (universal testing machine) and loaded at 1 kN at room temperature. The Vickers hardness tests were conducted on a Vickers microhardness tester (FV−700E) in the plane along the direction perpendicular to the welding line. The indenter load was 9.8 N and the loading time was 15 s. The microhardness measurements enclosed the heat affected zone (HAZ), thermomechanically affected zone (TMAZ),

NZ and areas of base metal (BM) adjoining the HAZ on both sides of the joint. Besides, the FESEM technique was also employed primarily to study the fracture surface of tensile specimens.

3 Results and discussion

3.1 Surface characterization

The flow path of the plasticized materials on both the AS and RS across the tool pin and the process of joining were studied and predicted. The welding joint that was conducted by T_1 tool pin profile shows some onion rings and flashes and the spacing of the layer in the onion ring pattern is equal to the distance of forward motion of the tool in one rotation (Fig. 2(a)). This prediction agrees with Refs. [16,17]. As seen in Fig. 2(b), the welded sample has a defect-free surface skin layer, which is an indicative of efficient material flow and constant pins depth. This joint was fabricated using the T_2 tool pin profile. According to Fig. 2(c), the welding joint that was accomplished by a T_3 tool pin profile shows some flashes on the RS, which results in flexible material passing through this side. This may attributed to the highest working pressure due to non constant surface level during the FSW process. The main reasons for welding defects in the FSW are attributed to the unstable sinker tip design. The best control of sinking during the welding process can provide a perfect welded joint as found in Ref. [18]. MERAN [18] reported that the pin depth of sinking is a critical factor and difficult to be controlled. The depth of sinking must be constant along the welding process. But, that is not possible to provide especially in the joint process of long plates unless the surfaces are smooth. Therefore, the preparation of surface before welding is a critical factor and must be paid attention. Based on this study and with regarding to Figs. 2(a) and (c), it can be concluded that the reason for the occurrence of welding flashes is the unstable pin depth.

The thickness of the recirculation material flow is also affected by the material properties, welding parameters and rate of heat transfering into the tool. This zone occupies large areas at high elevation planes due to great momentum transporting from the rotating shoulder [19]. In the transition zone, the material transfer occurs mainly on the RS. A flow reversal in the AS which is close to the pin leads to a stagnant zone. The significance of the lack material flow on the AS is related to the formation of defects [20]. Accordingly, it can be inferred that the flow of material across the pin adds another reason for welding flashes on the RS (Fig. 2(c)). However, the flow of material is affected by the tool pin geometry [5], then it can be concluded that there is the best possible tool pin profile in order to obtain defect free welds with smooth surfaces for the FSW process of 6061 aluminum alloy.

3.2 Macrostructural studies

Different levels of strain on both sides of AS and RS were reported in Ref. [21]. The material in the AS moves to oppose the plate motion and is exposed to a more shear stress than that in the RS. The material closed to the non consumable tool has a high plastic deformation and temperature gradients, which causes a higher deformation rate on the AS than on the RS. It results in a different flow, stress and temperature gradient. In contrast, different thermal cycles of these two sides induce different properties and precipitate distribution in the welding zones [22]. The recrystallized area in the TMAZ in alloys is called the NZ traditionally. The material deforms plastically in this region (i.e., dynamic recrystallization). However, the cross sectional macrostructures of all specimens are shown in Fig. 3. Except the T_3 specimen, the remaining specimens are defect-free in the surface roots of NZ. Defect-free NZ is an indication of efficient material flow around the tool pin. Inappropriate material flow causes the formation of defects in NZ. The tool shoulder is responsible for the material integration. Interestingly, the material integration is properly done only if the material was

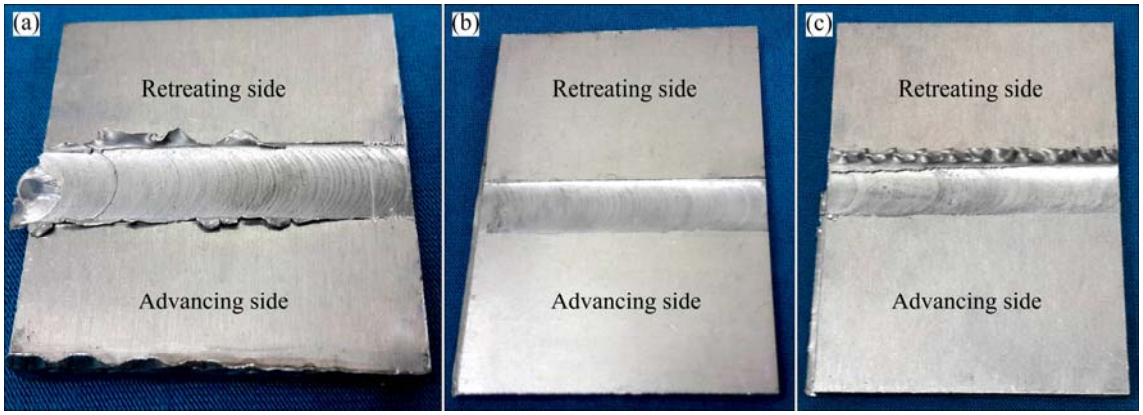

Fig. 2 Effect of tool pin geometry on weld surface quality: (a) Threaded tapered cylindrical pin T_1; (b) Triangular pin T_2; (c) Square pin T_3

plasticized well previously. As a consequence of having a similar small shoulder diameter, the material integrations are identical in all specimens. Therefore, the formation of void in the specimen fabricated with the T_3 tool pin profile can be attributed to an inefficient material flow around the tool pin which is due to the excessive heat input. This excessive heat increases the fluidity of metal and makes turbulent flow in the welded zone. This in turn results in the possibility of the formation of cavities [23].

The material transformation in the specimen fabricated with the T_3 tool pin profile only takes place in the regions close to the pin where the material flow is perfunctory. A superficial material flow around the pin results in a perfective stirring and subsequently partial material plasticization. This type of motion mechanism was also supported by BAHRAMI et al [24]. However, it can be concluded that other pin geometries produce a superficial material flow around the pin as well as thorough material plasticization within the NZ.

3.3 Microstructural observations

The FESEM images of the NZ of each specimen were obtained in a bright field (Fig. 4) to display the microstructures of all the joints for the comparison purpose. Figures 4(b), (d) and (f) show a magnified view of the surrounded regions in Figs. 4(a), (c) and (e), respectively. Figure 4(a) shows the microstructure at the

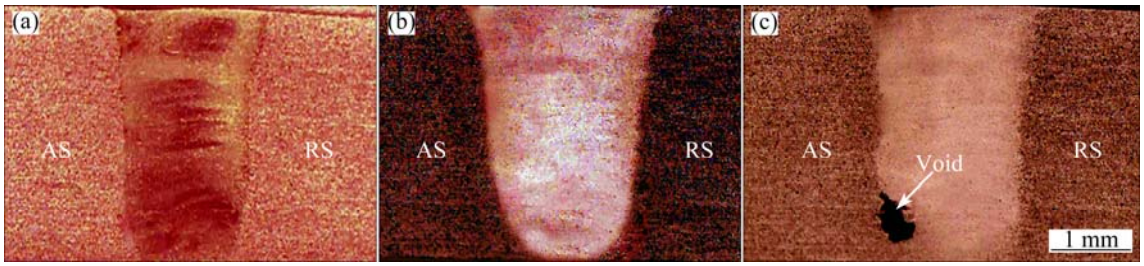

Fig. 3 Optical images of cross-sectional weld zone fabricated with different tool pin profiles: (a) Threaded tapered cylindrical pin T_1; (b) Triangular pin T_2; (c) Square pin T_3

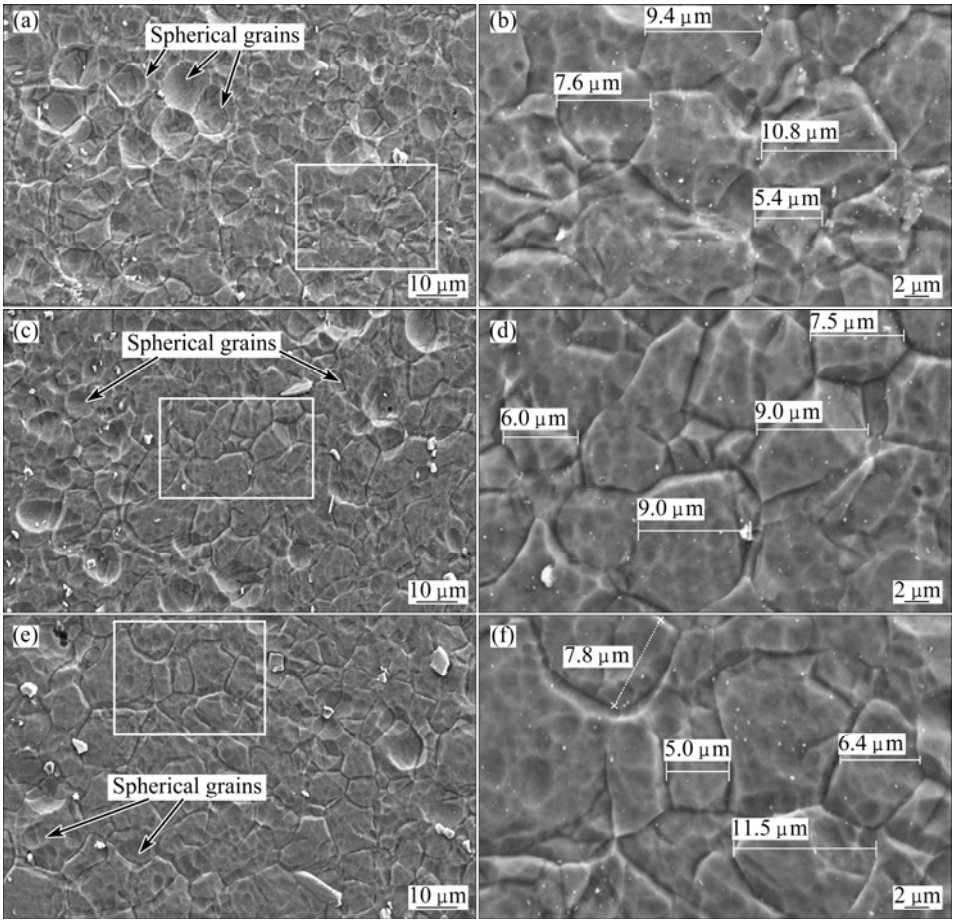

Fig. 4 FESEM micrographs of weld nugget zone of 6061 aluminium alloy joints friction stir welded with different tool pin profiles: (a, b) Threaded tapered cylindrical pin T_1; (c, d) Triangular pin T_2; (e, f) Square pin T_3

interface fabricated by T_1 tool pin profile. It can be observed that the NZ grains are refined and consist of spherical grains about 14 μm (Fig. 4(b))

The welding interface shown in Fig. 4(c) is fabricated with the T_2 tool pin profile. The grain distributed at the NZ is significantly more refined than that of T_1 specimen, probably because the contact area of the T_2 pin is less. Figure 4(d) also shows that some grains are approximately spherical in shape with an average size of ~9 μm. The frictional area between the T_2 pin and the material is limited to three flat faces, which is smaller than the contact area of T_1 pin. Furthermore, the bottom area of the T_2 pin is about 50% smaller than that of T_3 pin, while the bottom area of the T_1 pin is absolute zero. Ultimately, the less contact area of T_2 pin decreases the heat input into the NZ and generates more refined grains during the process of dynamic recrystallization [25].

Figure 4(e) shows the grain structure of the NZ of joint fabricated by the T_3 tool pin profile. Several grains in the NZ can be observed as spherical shapes under FESEM technique and it is also found that the average size of the grains is ~16 μm (Fig. 4(f)). The T_3 tool pin profile produces larger grains than the T_1 and T_2 tool pin profiles. The T_3 tool pin profile produces a pulsating stirring action in the flowing material due to its flat faces. In addition, four flat-faces of T_3 tool pin profile result in a large contact area and deformation. Thus, it can be deduced that the T_1 and T_3 specimens receive the minimum and maximum heat input, respectively. In this study, it can be inferred that the smaller dimension of T_2 tool pin profile gives finer grains and the desired heat input to the joint than other profiles of the pin. Moreover, it can be concluded that the small dimension side wall of the T_2 pin can produce spherical grains.

3.4 Effect of tool pin profiles on temperature and grain size

The temperatures around the tool pin during the FSW process were measured and are shown in Fig. 5. The relationship between different types of tool pin profiles and the grain size of the three joints are represented in Fig. 6. The maximum grain size value of the FSW joint is achieved when the joint is fabricated with the T_3 tool pin profile, while the minimum grain size is obtained when the joint is fabricated with the T_2 tool pin profile. Accordingly, it can be concluded that the T_2 tool pin profile gives finer grains than the T_1 and T_3 tool pin profiles when the weld joint is conducted under the same welding parameters. HIRATA et al [25] and ILANGOVAN et al [26] reported that the grain size in the NZ decreases when the friction heat input decreases. Hence, it can be inferred that the T_2 tool pin profile decreases the heat generation due to its small contact area, thereby, more grain refinement is achieved. In other words, this phenomenon reflects the hegemony of heat input factor to the stirring action of the pin. However, smaller grain size values of the joint fabricated by T_2 tool pin profile have particular correlation with the heat input factor and the stirring action of the pin.

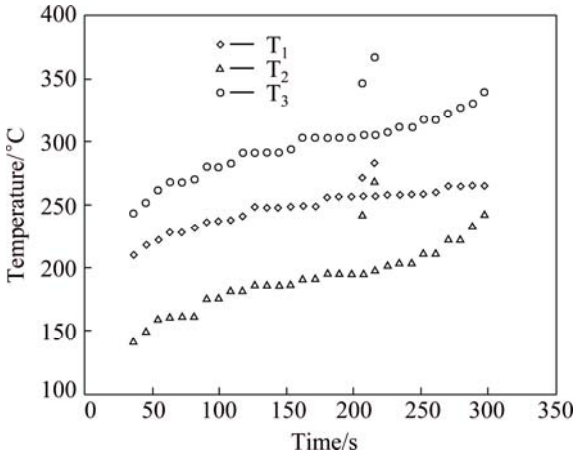

Fig. 5 Transient temperatures sensed by thermocouples for different tool pin profiles

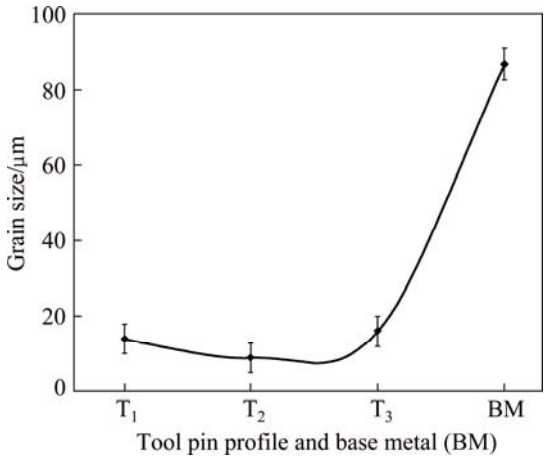

Fig. 6 Effect of different tool pin profiles on grain size of 6061 aluminium alloy joints

3.5 Effect of tool shoulder diameter

Figure 7 shows the effect of the tool shoulder diameters on the temperature distributions in the NZ and in the area adjacent to the shoulder, which were obtained by ANSYS software, and explains the temperature distribution through the readable temperature scales. It is evident from Fig. 7 that when the welded region is conducted with a tool shoulder diameter of 9 mm, the heat generated by friction is significantly less as compared with that generated by the tool shoulder diameter of 13 mm. In contrast, when the diameter is somewhat small, the heat will be focused on the small contact area beneath the shoulder. This in turn, less heat will be transferred by conducting to the HAZ region, causing an increase of mechanical properties as some volume fraction of precipitate remains without dissolving.

Moreover, if the tool shoulder diameter is large, then the heat input will be high due to the large contact area. These findings are in good agreement with Refs. [25,27].

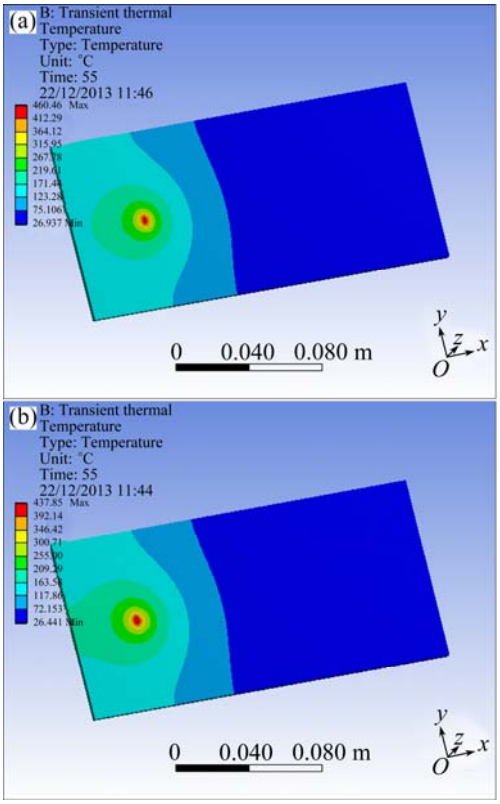

Fig. 7 Temperature distribution in FSW of aluminum plate with different tool shoulder diameters: (a) 13 mm; (b) 9 mm

3.6 X-ray diffraction (XRD) analysis

Figure 8 shows the X-ray diffraction patterns of the NZ for all joints that were fabricated by the different tool pin profiles. The relevant parameters corresponding to the diffraction peaks in the diagram have been computed using X' Pert High Score Plus software, which indicates that the aluminum alloy as a cubic structure. The relative intensities in XRD peaks of 6061 aluminum alloy match with the reference code 98-006-2706. The maximum diffraction peaks of aluminum are obvious in Fig. 8. In addition, according to the results during the FSW process, alloy metal or intermetallic compounds are not observed. These intermetallic compounds give high hardness and fragility to the NZ at the same time. If they are found in large quantities, they will decrease the tensile strength. The present work focuses on decreasing the heat input to the welding joint as much as possible using a small tool pin profile and a small shoulder diameter, to prevent the formation of intermetallic compounds. High temperatures (i.e., High heat input) result in the growth of intermetallic compounds [28].

The XRD data in Table 2 show the changes in calculated density, crystallite size and lattice parameters

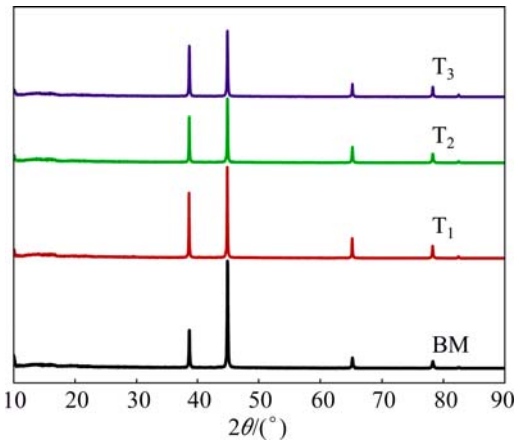

Fig. 8 XRD patterns of 6061 aluminum alloy before and after FSW with different tool pin profiles

Table 2 XRD data of 6061 aluminum alloy joints fabricated by different pin profiled tools compared with base metal (BM)

Material	Density (calculated)/ ($g \cdot cm^{-3}$)	Crystallite size/nm	Lattice parameters (a,b,c)/nm
T1 specimen	2.6892	84.81	0.40534
T2 specimen	2.6901	72.04	0.40537
T3 specimen	2.6907	114.33	0.40541
BM	2.6883	64.87	0.40546

of the joints which were fabricated with different tool pin profiles and compared with those of the BM. The data obtained from the XRD analysis shows more changes, indicating that the crystallite size is influenced significantly during the FSW process. The scatter in the results of the crystallite size shows different values with different tool pin profiles, but in general the results remain very close except the crystallite size of the joint that was fabricated by the T_3 tool pin profile. It can be noticed that the crystallite size of the joint fabricated by the T_1 pin almost matches to that of the joint fabricated by the T_2 tool pin profile and the BM. Compared with the initial calculated density in the BM (2.6883 g/cm^3), which can be found in the different joints, a slight increase of calculated density is observed at different joints fabricated with different tool pin profiles during the FSW. The calculated density and lattice parameters of the grain structure can significantly influence the strain-hardening behavior associated with the tool pin profiles during deformation. Therfore, this variable observation of transient microstructure is important in understanding the complicated FSW process, which includes the plastic deformation and dynamic recrystallization with changed tool pin profiles.

3.7 Mechanical properties

3.7.1 Tensile test analysis of joints

Several microstructural factors, such as grains size,

dislocation density, and interaction between the BM and the tool pin profiles, influence the tensile strength [29]. The tensile strength of the FSW joints was evaluated and the data are shown in Table 3. As seen from the results, the welded joint fabricated by the T_3 tool pin profile exhibits an inferior tensile strength. This result is related to the presence of voids in the NZ. The void is considered as a very serious defection which affects the mechanical properties remarkably and decreases the tensile strength sharply [30]. The highest value of tensile strength is obtained with the joint fabricated by the T_2 tool pin profile. According to Hall−Petch equation, the decrease of grain size results in the improvement of tensile strength [25]. Therefore, the highest tensile strength presumably occurs at the joint fabricated by the T_2 tool pin profile because the T_2 specimen has the smallest grain size. Similarly, the tensile properties of the joint fabricated by the T_1 tool pin profile almost matches with those of joint fabricated by the T_2 tool pin profile. The ductility in terms of elongation to rupture and the tensile strength of joint fabricated by T_3 tool pin profile reduce. The experimental results show that the fracture failure occurs on the AS of the weld joints. However, it can be attributed to defects, because usually the AS is weaker than the RS [31].

Table 3 Results of tensile test

Pin tool profile	Tensile strength/MPa	Elongation/%
T_1	142.656	3.2
T_2	149.483	3.7
T_3	133.8	2.9

3.7.2 Vickers microhardness test

The average Vickers microhardness values for the similar workpieces and single pass weld were measured transversely and the measurement direction was perpendicular to the direction of the weld line. The microhardness profiles of the specimens are represented in Fig. 9. It can be seen that the microhardness in the area of NZ is significantly higher than that of TMAZ and HAZ, but it is lower than that of the BM. The variation in the microhardness between welding zones and the BM is due to closely convoluted grain sizes and heat input. This feature is also documented in Ref. [32]. Moreover, the microhardness distribution is different from the center line, and these differences are caused by grain size variation in different welded regions [33,34]. The increase of temperature results in the growth of the grains, and during the FSW, the grains undergo intense plastic deformation within the processed zone, resulting in the grain refinement due to the dynamic recrystallization. So, the dynamically recrystallized grains followed by static recovery and subsequent grain development during the cooling of microstructures are obtained.

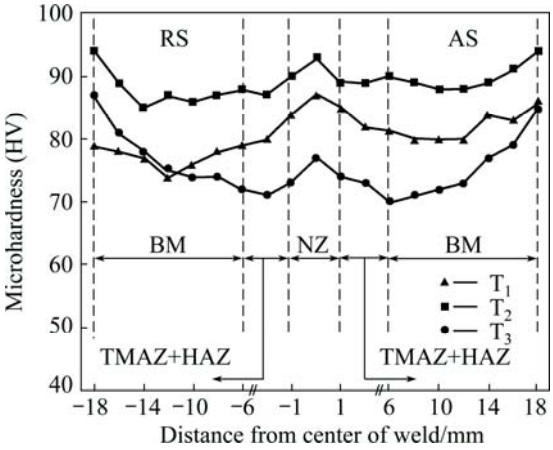

Fig. 9 Microhardness of 6061 aluminum alloy joints welded by different tool pin profiles

The grain size increases continuously with increasing temperature, which is caused by an increase of the rotational speed or the shoulder diameter [28]. The microhardness in the NZ increases when the frictional heat input decreases. The grain size in the NZ decreases when the friction heat input decreases [25]. Here, it can be concluded that, a high heat input results in an increase of grain size, and also causes the weakness in the HAZ region. The controlling of the welding parameters, particularly the rotational speed, the tool pin profiles and the shoulder diameter can yield a high level of welding quality and an improvement of HAZ properties. Another cause for variation in microhardness between the welding zones and the BM is the precipitates, because in alloys such as 6061 aluminum alloy, the main precipitate is Mg_5Si_6 which is stable at temperatures lower than 200 °C [35]. The nugget microhardness and their center revival are due to the dynamic recrystallization of a very fine grain structure. Hence, it can be concluded that the significant precipitate variation in the weld regions have a significant effect on the variations of microhardness.

It is also observed in Fig. 9 that there is a higher microhardness on the AS than on the RS through the TMAZ and HAZ due to the existence of more strain and plastic deformation caused by the welding tool which results in remarkable refining effects. According to Hall−Petch equation [25], finer grains are associated with higher hardness content. As indicated in Fig. 9, the microhardness of the HAZ gives improved value. The results exhibit a significantly lower heat generation, probably due to the effects of small welding tool dimensions. The slight increase of surface microhardness values in the HAZ region indicates that there is no temperature high enough during the welding to dissolve

all precipitates, and this finding is also supported by UZUN et al [21]. In this investigation, it is observed that the small tool shoulder diameter and tool pin lead to the formation of a narrow HAZ region with ~1.5 mm in width. THOMAS and NICHOLAS [36] have reported that if the shoulder diameter is large, the heat generated by friction will be high due to the large contact area, resulting in wide TMAZ and HAZ. Accordingly, it can be inferred that in the case of small shoulder diameter and pin profiles, less amount of heat will be generated by friction and conducted to HAZ. This process results in a narrow HAZ and desired level of softening, and thereby increases the microhardness value.

3.8 Fractograph

It is generally known that the fusion welding of aluminum alloys is accompanied by the defects like porosity, inclusion, solidification and cracks, and these defects deteriorate the quality of the weld. The FSW joints are known to be free from these defects since melting does not take place during the welding process and the metals are joined in the solid state due to the heat generated by the friction and the flow of metal by the stirring action. But, the FSW joints are prone to other defects like pin holes, tunnel defects and cracks. However, the fracture surface failure of the tensile specimens is captured using the FESEM technique to detect the fracture pattern defects. In spite of the T_2 specimen which is failed in the NZ, the remaining specimens are fractured in the TMAZ at the AS. However, the presence of voids in the NZ or in the TMAZ is the reasons for the failure of these region. Figure 10 shows the uneven surface accompanied with fibrous tedious appearance which was fabricated by the T_1 tool pin profile, and shows characteristics of brittle fracture. Figure 11 also shows an uneven and concave fracture surface with the presence of some deep dimples. This fracture surface exhibits a ductile fracture mode and is suggested to improve the tensile ductility of this specimen. In contrary, a brittle type fracture mode is found in the joint which is fabricated by the T_3 tool pin profile, (Fig. 12). Figure 12 shows an uneven surface and striations, which may be attributed to the groove corresponding to the tunnel in the cross section [37].

From the results of FESEM analysis, it can be concluded that the genesis of a defect-free weld is a function of the tool pin profile. This conclusion was also affirmed by Ref. [6]. These three conditions are selected for fractographic analysis to investigate the factor of heat input because this factor is the main feature determining the tensile strength of the joints and the difference of heat input between these conditions is the most marginal [38]. As seen in Fig. 11, the contact area of T_2 tool pin profile

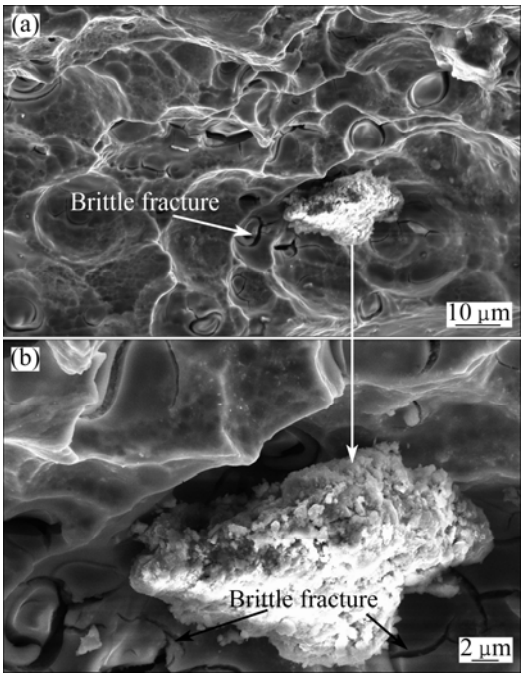

Fig. 10 FESEM micrographs of 6061 aluminum alloy joint after tensile test using T_1 tool pin with different magnifications

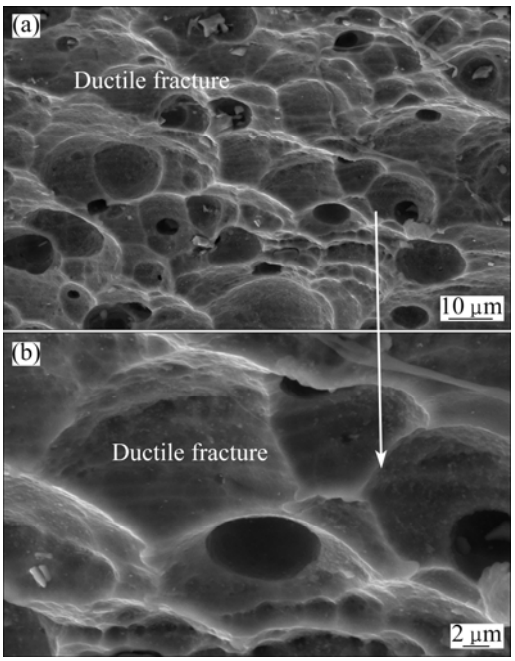

Fig. 11 FESEM micrographs of 6061 aluminum alloy joint after tensile test using T_2 tool pin with different magnifications

is less than those of T_1 and T_3 tool pin profiles, then the ductile fracture appears in this joint. As shown in Figs. 10 and 12, due to the excess of heat, there are brittle fractures on the fractural surface. Accordingly, the tensile strengths of T_1 and T_3 specimens are less than that of T_2 specimen. All the FESEM fractographs are in good accordance with the corresponding elongation values mentioned in Table 3.

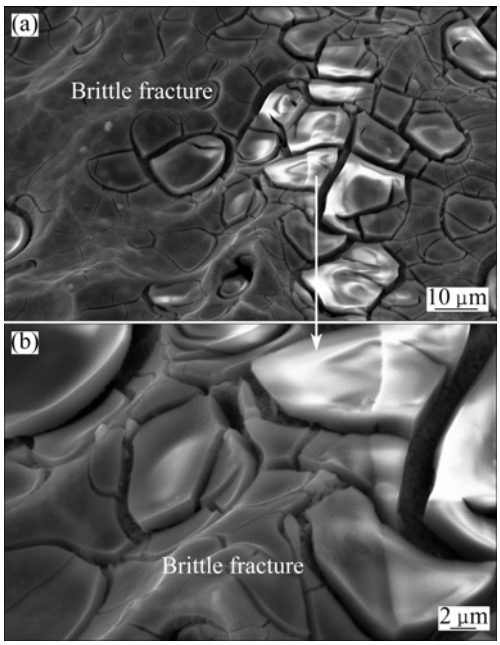

Fig. 12 FESEM micrographs of 6061 aluminum alloy joint after tensile test using T_3 tool pin with different magnifications

4 Conclusions

1) The geometry and dimension of the welding tool used in the FSW process influence the mechanical properties of the joints.

2) The best mechanical properties are obtained for the FSW joint produced by a triangular tool pin profile when compared with their counterparts. Moreover, the less pulsating action experienced in the NZ of triangular tool pin profile produces fine grains.

3) The lowest tensile strength and microhardness are recorded for the specimen fabricated with square tool pin, which are mostly related to the interfacial defects and grain size, respectively.

4) In the case of a small shoulder diameter and tool pin profiles, less amount of heat is generated by friction and passes to the HAZ region. This process results in a narrow HAZ and a desired level of softening which results in increasing the microhardness.

5) The fractured surfaces of tensile specimens are characterized as brittle fractures in the joints friction stir welded with threaded tapered cylindrical pin and square pin due to the effect of excess heat generated during the FSW process. The ductile fractures are observed on the fractured surface of the joint produced with low heat input (i.e., the joints fabricated by the triangular tool pin profile).

Acknowledgements

This work was supported by the grant No. 9001-00338 of the Universiti Malaysia Perlis (UniMAP). The Authors gratefully acknowledge the outstanding support provided by the staff in the School of Materials Engineering in UniMAP, the Centre for Low Carbon Transport and Institute for Vehicle System Engineering in Universiti Teknologi Malaysia (UTM) and the School of Materials Engineering and Mineral Resources in Universiti Sains Malaysia (USM).

References

[1] THOMAS W, NICHOLAS E, NEEDHAM J, MURCH M, TEMPLESMITH P, DAWES C. International patent application PCT/GB92/02203 and GB patent application: US, 9125978.8 [P]. 1991−12.

[2] STARON P, KOCAK M, WILLIAMS S, WESCOTT A. Residual stress in friction stir-welded Al sheets [J]. Physica B: Condensed Matter, 2004, 350: 491−493.

[3] CHEN Y, LIU H, FENG J. Friction stir welding characteristics of different heat-treated-state 2219 aluminum alloy plates [J]. Materials Science and Engineering A, 2006, 420: 21−25.

[4] SUN Y, FUJII H. The effect of SiC particles on the microstructure and mechanical properties of friction stir welded pure copper joints [J]. Materials Science and Engineering A, 2011, 528: 5470−5475.

[5] LIU H, CHEN Y, FENG J. Effect of zigzag line on the mechanical properties of friction stir welded joints of an Al−Cu alloy [J]. Scripta Materialia, 2006, 55: 231−234.

[6] ELANGOVAN K, BALASUBRAMANIAN V. Influences of tool pin profile and welding speed on the formation of friction stir processing zone in AA2219 aluminium alloy [J]. Journal of Materials Processing Technology, 2008, 200: 163−175.

[7] FARAJI G, ASADI P. Characterization of AZ91/alumina nanocomposite produced by FSP [J]. Materials Science and Engineering A, 2011, 528: 2431−2440.

[8] AZIZIEH M, KOKABI A, ABACHI P. Effect of rotational speed and probe profile on microstructure and hardness of AZ31/Al_2O_3 nanocomposites fabricated by friction stir processing [J]. Materials & Design, 2011, 32: 2034−2041.

[9] ZHANG D, SUZUKI M, MARUYAMA K. Microstructural evolution of a heat-resistant magnesium alloy due to friction stir welding [J]. Scripta Materialia, 2005, 52: 899−903.

[10] FENG A, MA Z. Enhanced mechanical properties of Mg−Al−Zn cast alloy via friction stir processing [J]. Scripta materialia, 2007, 56: 397−400.

[11] WOO W, CHOO H, BROWN D, LIAW P, FENG Z. Texture variation and its influence on the tensile behavior of a friction-stir processed magnesium alloy [J]. Scripta materialia, 2006, 54: 1859−1864.

[12] CHANG C, DU X, HUANG J. Achieving ultrafine grain size in Mg–Al–Zn alloy by friction stir processing [J]. Scripta Materialia, 2007, 57: 209−212.

[13] BHARGAVA G, YUAN W, WEBB S, MISHRA R S. Influence of texture on mechanical behavior of friction-stir-processed magnesium alloy [J]. Metallurgical and Materials Transactions A, 2010, 41: 13−17.

[14] CHANG C, DU X, HUANG J. Producing nanograined microstructure in Mg–Al–Zn alloy by two-step friction stir processing [J]. Scripta Materialia, 2008, 59: 356−359.

[15] YUAN W, PANIGRAHI S, SU J Q, MISHRA R. Influence of grain size and texture on Hall–Petch relationship for a magnesium alloy [J]. Scripta Materialia, 2011, 65: 994−997.

[16] SUTTON M, YANG B, REYNOLDS A, TAYLOR R. Microstructural studies of friction stir welds in 2024-T3 aluminum [J]. Materials Science and Engineering A, 2002, 323: 160−166.

[17] KRISHNAN K. On the formation of onion rings in friction stir welds [J]. Materials Science and Engineering A, 2002, 327: 246−251.
[18] MERAN C. The joint properties of brass plates by friction stir welding [J]. Materials & Design, 2006, 27: 719−726.
[19] JATA K, SEMIATIN S. Continuous dynamic recrystallization during friction stir welding of high strength aluminum alloys [J]. Scripta Materialia, 2000, 43: 743−749.
[20] SEIDEL T, REYNOLDS A. Two-dimensional friction stir welding process model based on fluid mechanics [J]. Science and Technology of Welding & Joining, 2003, 8: 175−183.
[21] UZUN H, DALLE DONNE C, ARGAGNOTTO A, GHIDINI T, GAMBARO C. Friction stir welding of dissimilar Al 6013-T4 to X5CrNi18-10 stainless steel [J]. Materials & Design, 2005, 26: 41−46.
[22] LIU G, MURR L, NIOU C, MCCLURE J, VEGA F. Microstructural aspects of the friction-stir welding of 6061-T6 aluminum [J]. Scripta Materialia, 1997, 37: 355−361.
[23] GAAFER A, MAHMOUD T, MANSOUR E. Microstructural and mechanical characteristics of AA7020-O Al plates joined by friction stir welding [J]. Materials Science and Engineering A, 2010, 527: 7424−7429.
[24] BAHRAMI M, BESHARATI GIVI M K, DEHGHANI K, PARVIN N. On the role of pin geometry in microstructure and mechanical properties of AA7075/SiC nano-composite fabricated by friction stir welding technique [J]. Materials & Design, 2014, 53: 519−527.
[25] HIRATA T, OGURI T, HAGINO H, TANAKA T, CHUNG S W, TAKIGAWA Y, HIGASHI K. Influence of friction stir welding parameters on grain size and formability in 5083 aluminum alloy [J]. Materials Science and Engineering A, 2007, 456: 344−349.
[26] ILANGOVAN M, BOOPATHY S R, BALASUBRAMANIAN V. Microstructure and tensile properties of friction stir welded dissimilar AA6061–AA5086 aluminum alloy joints [J]. Transactions of Nonferrous Metals Society of China, 2015, 25(4): 1080−1090.
[27] ZHANG Zhao, WU Qi, ZHANG Hong-wa. Numerical studies of effect of tool sizes and pin shapes on friction stir welding of AA2024-T3 alloy [J]. Transactions of Nonferrous Metals Society of China, 2014, 24(10): 3293−3301.
[28] SATO Y S, URATA M, KOKAWA H. Parameters controlling microstructure and hardness during friction-stir welding of precipitation-hardenable aluminum alloy 6063 [J]. Metallurgical and Materials Transactions A, 2002, 33: 625−635.
[29] BARMOUZ M, ASADI P, BESHARATI GIVI M, TAHERISHARGH M. Investigation of mechanical properties of Cu/SiC composite fabricated by FSP: Effect of SiC particles' size and volume fraction [J]. Materials Science and Engineering A, 2011, 528: 1740−1749.
[30] ZHAO Y H, LIN S B, WU L, QU F X. The influence of pin geometry on bonding and mechanical properties in friction stir weld 2014 Al alloy [J]. Materials Letters, 2005, 59: 2948−2952.
[31] LIU H, FUJII H, MAEDA M, NOGI K. Tensile properties and fracture locations of friction-stir-welded joints of 2017-T351 aluminum alloy [J]. Journal of Materials Processing Technology, 2003, 142: 692−696.
[32] BAHRAMI M, DEHGHANI K, BESHARATI GIVI M K. A novel approach to develop aluminum matrix nano-composite employing friction stir welding technique [J]. Materials & Design, 2014, 53: 217−225.
[33] YAN Yong, ZHANG Da-tong, QIU Cheng, ZHANG Wen. Dissimilar friction stir welding between 5052 aluminum alloy and AZ31 magnesium alloy [J]. Transactions of Nonferrous Metals Society of China, 2010, 20(S2): s619−s623.
[34] SOMASEKHARAN A, MURR L. Microstructures in friction-stir welded dissimilar magnesium alloys and magnesium alloys to 6061-T6 aluminum alloy [J]. Materials Characterization, 2004, 52: 49−64.
[35] BRATLAND D, GRONG Ø, SHERCLIFF H, MYHR O, TJØTTA S. Overview No.124 Modelling of precipitation reactions in industrial processing [J]. Acta Materialia, 1997, 45: 1−22.
[36] THOMAS W, NICHOLAS E. Friction stir welding for the transportation industries [J]. Materials & Design, 1997, 18: 269−273.
[37] UDAY M B, AHMAD FAUZI M N, ZUHAILAWATI H, ISMAIL A B. Effect of welding speed on mechanical strength of friction welded joint of YSZ–alumina composite and 6061 aluminum alloy [J]. Materials Science and Engineering A, 2011, 528: 4753−4760.
[38] DEHGHANI M, MOUSAVI S A, AMADEH A. Effects of welding parameters and tool geometry on properties of 3003-H18 aluminum alloy to mild steel friction stir weld [J]. Transactions of Nonferrous Metals Society of China, 2013, 23(7): 1957−1965.

小搅拌针形状对搅拌摩擦焊 6061 铝合金显微组织和力学性能的影响

H. I. DAWOOD[1,2], Kahtan S. MOHAMMED[1], Azmi RAHMAT[1], M. B. UDAY[3]

1. School of Materials Engineering, Universiti Malaysia Perlis, Taman Muhibah-Jejawi-Arau, Perlis 02600, Malaysia;
2. Department of Chemical Engineering, College of Engineering, University of AL-Qadisiya, AL-Qadisiya, Iraq;
3. Centre for Low Carbon Transport in Cooperation with Imperial College London, Institute for Vehicle System Engineering, Universiti Teknologi Malaysia, Skudai 81310, Malaysia

摘　要：研究小搅拌针形状对 6061 铝合金搅拌摩擦焊接头的显微组织和力学性能的影响。采用 3 种不同形状的搅拌针：螺纹锥形圆柱形(T1)、三角形(T2)和正方形(T3)。结果表明：不同形状的搅拌针会显著地影响焊接接头的性能。相对于使用其他形状的搅拌针，使用三角形搅拌针能获得最好的冶金和力学焊接性能。此外，使用正方形搅拌针制备的搅拌摩擦焊接头具有最低的拉伸强度和显微硬度。更小的搅拌针形状和轴肩直径导致热影响区域变窄和一定程度的软化。断口分析结果表明，不同形状的搅拌针焊接也能影响接头。断裂面显示三角形搅拌针制备的样品在拉伸试验中以韧性断裂形式失效，而在用其他形状的搅拌针(T1 和 T2)制备的接头中观察到了脆性断裂。

关键词：搅拌摩擦焊；小搅拌针形状；力学性能；铝合金；晶粒尺寸

(Edited by Mu-lan QIN)